

# The Finite-Size Scaling Study of the Specific Heat and the Binder Parameter of the Two-Dimensional Ising Model for the Fractals Obtained by Using the Model of Diffusion-Limited Aggregation

Ziya Merdan<sup>a</sup>, Mehmet Bayirli<sup>b</sup>, and Mustafa Kemal Ozturk<sup>c</sup>

<sup>a</sup> Faculty of Arts and Sciences, Department of Physics, Kirikkale University, Kirikkale, Turkey

<sup>b</sup> Faculty of Arts and Sciences, Department of Physics, Balikesir University, Balikesir, Turkey

<sup>c</sup> Department of Mineral Analysis and Technology, MTA, Ankara, Turkey

Reprint requests to Z. M.; E-mail: zmerdan1967@hotmail.com

Z. Naturforsch. **64a**, 849–854 (2009); received March 6, 2009 / revised May 1, 2009

The two-dimensional Ising model with nearest-neighbour pair interactions is simulated on the Creutz cellular automaton by using the finite-size lattices with the linear dimensions  $L = 80, 120, 160, \text{ and } 200$ . The temperature variations and the finite-size scaling plots of the specific heat and the Binder parameter verify the theoretically predicted expression near the infinite lattice critical temperature. The approximate values for the critical temperature of the infinite lattice  $T_c = 2.287(6)$ ,  $T_c = 2.269(3)$ , and  $T_c = 2.271(1)$  are obtained from the intersection points of specific heat curves, Binder parameter curves, and the straight line fit of specific heat maxima, respectively. These results are in agreement with the theoretical value ( $T_c = 2.269$ ) within the error limits. The values obtained for the critical exponent of the specific heat,  $\alpha = 0.04(25)$  and  $\alpha = 0.03(1)$ , are in agreement with  $\alpha = 0$  predicted by the theory. The values for the Binder parameter by using the finite-size lattices with the linear dimension  $L = 80, 120, 160, \text{ and } 200$  at  $T_c = 2.269(3)$  are calculated as  $g_L(T_c) = -1.833(5)$ ,  $g_L(T_c) = -1.834(3)$ ,  $g_L(T_c) = -1.832(2)$ , and  $g_L(T_c) = -1.833(2)$ , respectively. The value of the infinite lattice for the Binder parameter,  $g_L(T_c) = -1.834(11)$ , is obtained from the straight line fit of  $g_L(T_c) = -1.833(5)$ ,  $g_L(T_c) = -1.834(3)$ ,  $g_L(T_c) = -1.832(2)$ , and  $g_L(T_c) = -1.833(2)$  versus  $L = 80, 120, 160, \text{ and } 200$ , respectively.

*Key words:* Ising Model; Cellular Automaton; Finite-Size Scaling; Scanning Method.

*PACS numbers:* 05.50.+q, 64.60. Cn, 75.40. Cx, 75.40. Mg

## 1. Introduction

The application of fractal concepts, first introduced by Mandelbrot et al. to describe complex natural shapes and structures as well as mathematical sets and functions having an intricately irregular form, has been studied [1–4]. The aggregation of particles to form cluster has, for a long time, been one of the central phenomena in natural science with important implications for physical problems such as air pollution, dielectric breakdown, bacterial colony growth, and natural formations (snowflakes and manganese dendrites). The model allow an exploration of the process of pattern formation in real physical systems which is based mostly on the model of diffusion-limited aggregation. This model describes the most important morphology patterns observed in various non-equilibrium systems, such as diffusion-limited aggregation-like, dendrite, needle, tree-like, dense-branching, compact, stingy, spiral, and chiral structures [5–14].

The Creutz cellular automaton [15] has simulated the two dimensional Ising model successfully near the critical region, and has reproduced its critical exponents within the framework of the finite-size scaling theory [16, 17]. This algorithm is an order of magnitude faster than the conventional Monte Carlo method and it does not need high quality random numbers. These features of the Creutz cellular automaton would make the Ising model simulations in higher dimensions more practical. Compared to Q2R cellular automaton [18] it has the advantage of allowing the specific heat to be computed from the internal energy fluctuations.

The purpose of this study is to test the finite-size scaling study of the specific heat and the Binder parameter of the two-dimensional Ising model for the fractals obtained by using the model of diffusion-limited aggregation. However, the test studies in  $d = 2$  dimensions are not available. The simulations are carried out on the Creutz cellular automaton, which has success-

fully arisen as an alternative research tool for Ising models in the dimensionalities  $2 \leq d \leq 8$  [19].

The model is described in Section 2, the results are discussed in Section 3, and a conclusion is given in Section 4.

## 2. Model

In the model of diffusion-limited aggregation, the central particle is placed in the closed square lattice. Another new particle is started to move on the edge of the lattice site. If this fragment passes by the neighbouring site of the central particle during the random moving, it fixes there. The same conditions are applied to the other particles. However, when the particle or a group of particles goes out of the determined lattice site, at which the particle is cancelled, then another particle is suggested. The operation is repeated until the suggested number of particles in the aggregate, i. e. the behaviour of a particle or a particle group, is obtained.

At the Creutz cellular automaton, four binary bits are associated with each site of the lattice. The value for each site is determined from its value and those of its nearest neighbours at the previous time step. The updating rule, which defines a deterministic cellular automaton, is as follows: Of the four binary bits on each site, the first one is the Ising spin  $B_i$ . Its value may be “0” or “1”. Ising spin energy (internal energy) of the lattice,  $H_I$ , is given (in units of the nearest neighbour coupling constant  $J$ ) by

$$H_I = -J \sum_{\langle i,j \rangle} S_i S_j, \quad (1)$$

where  $S_i = 2B_i - 1$ , and  $\langle i, j \rangle$  denotes the sum over all nearest neighbour pairs of sites. The second and the third bits are for the momentum variable conjugate to the spin (the demon). These two bits form an integer which can take on the value 0, 1, 2, or 3. The kinetic energy (in units of  $J$ ) associated with the demon can take on four times these integer values. The total energy

$$H = H_I + H_K \quad (2)$$

is conserved; here  $H_K$  is the kinetic energy of the lattice. For a given total energy the system temperature  $T$  (in units of  $J/k_B$  where  $k_B$  is the Boltzmann constant) is obtained from the average value of the kinetic energy. The fourth bit provides a checkerboard style updating, and so it allows the simulation of the

Ising model on a cellular automaton. The black sites of the checkerboard are updated and then their color is changed into white: the white sites are changed into black without being updated.

The updating rules for the spin and the momentum variables are as follows: For a site to be updated its spin is flipped and the change in the Ising energy (internal energy),  $H_I$ , is calculated. If this energy change is transferable to or from the momentum variable associated with this site, such that the total energy,  $H$ , is conserved, then this change is done and the momentum is appropriately changed. Otherwise the spin and momentum are not changed.

As the initial configuration all spins are taken ordered (up or down). The initial kinetic energy is randomly given to the lattice via the second bits of the momentum variables in the white sites. The quantities computed are averages over the lattice and the number of time steps during which the cellular automaton develops.

The simulations are carried out on simple hypercubic lattices  $L^2$  of linear dimensions  $80 \leq L \leq 200$  with periodic boundary conditions by using two-bit demons. The cellular automaton develops  $9.6 \cdot 10^5$  ( $L = 80, 120, 160, 200$ ) sweeps for each run with seven runs for each total energy.

## 3. Results and Discussion

The fractals obtained by using the model of diffusion-limited aggregation are illustrated in Figure 1 for the lattice with  $L = 80, 120, 160$ , and  $200$ . In  $d = 2$  dimension, the finite-size scaling relation for the specific heat  $C_L$  is derived below [16, 20]. The finite-size scaling relations for the critical temperatures and the free-energy density are given as [16, 20]:

$$(T_c - T_c(L)) \propto L^{-1/\nu}, \quad (3)$$

$$f_L = L^{-d} F(tL^{y_t}, hL^{y_h}), \quad h \rightarrow 0, \quad L \rightarrow \infty, \quad (4)$$

where  $y_t = \frac{1}{\nu}$  and  $y_h = \frac{\Delta}{\nu}$ , with  $d\nu = 2 - \alpha$  and  $\Delta = \gamma + \beta$ ,  $t = (T - T_c)/T_c$  is the reduced temperature with  $t > 0$  for  $T > T_c$  and  $t < 0$  for  $T < T_c$ ,  $h$  is the reduced external magnetic field,  $\alpha$ ,  $\beta$ , and  $\gamma$  are the critical exponents for the specific heat, order parameter, and the magnetic susceptibility of the infinite lattice, respectively. Thus,  $f_L$  takes the following form:

$$f_L = L^{-d} F(tL^{1/\nu}, hL^{(\gamma+\beta)/\nu}). \quad (5)$$

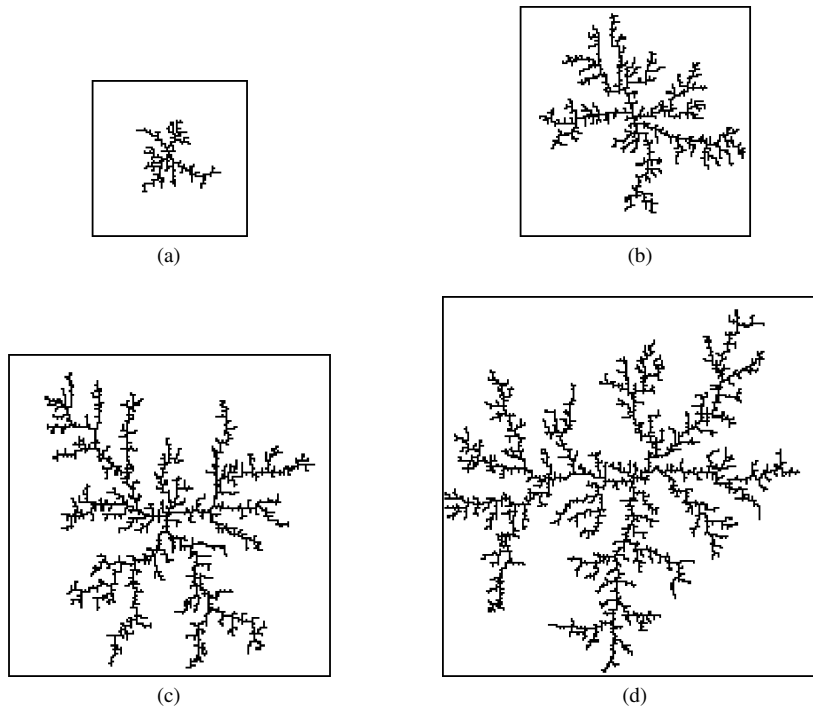


Fig. 1. Images of the fractals obtained by using the model of diffusion-limited aggregation for lattices with the linear dimensions (a)  $L = 80$ , (b)  $L = 120$ , (c)  $L = 160$ , and (d)  $L = 200$ .

Table 1. The critical temperature and the maximum values of the specific heat for the finite lattices and the values  $T_c = 2.269$ .

$L$	$T_c^C(L)$	$C_L^{\max}$	$C_L(T_c)$
80	2.2624(3)	0.575(6)	0.561(12)
120	2.2646(2)	0.593(12)	0.574(14)
160	2.2669(2)	0.598(24)	0.591(22)
200	2.2678(3)	0.602(39)	0.598(40)

By using the definition  $C_L = -\frac{\partial^2 f_L}{\partial t^2}$  the following equation is obtained:

$$C_L = L^{\alpha/\nu} F(tL^{1/\nu}, hL^{(\gamma+\beta)/\nu}). \tag{6}$$

Since  $\alpha = 0$ ,  $\beta = \frac{1}{8}$ , and  $\gamma = \frac{7}{4}$  in  $d = 2$  dimension,  $C_L$  takes the following form:

$$C_L = F(tL^{1/\nu}, hL^{(\gamma+\beta)/\nu}). \tag{7}$$

At  $h = 0$  (7) becomes

$$C_L = F(tL^{1/\nu}), \tag{8}$$

where  $F = F(x)$  is the finite-size scaling function (the shape function) for the specific heat. This is the relation to be tested. The plots of  $C_L$  versus temperature ( $T$ )

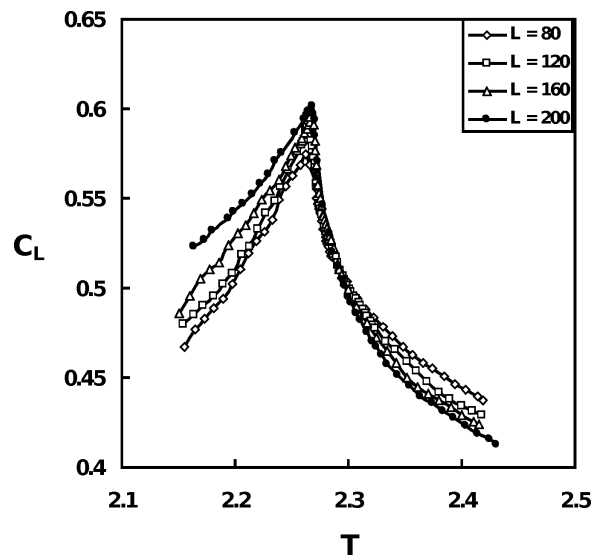


Fig. 2. Specific heat  $C_L$  as a function of the temperature  $T$  for sizes  $80 \leq L \leq 200$ .

and corresponding temperatures of specific heat maxima ( $T_c^C(L)$ ) listed in Table 1 versus  $L^{-1/\nu}$  are illustrated in Figures 2 and 3, respectively. The intersec-

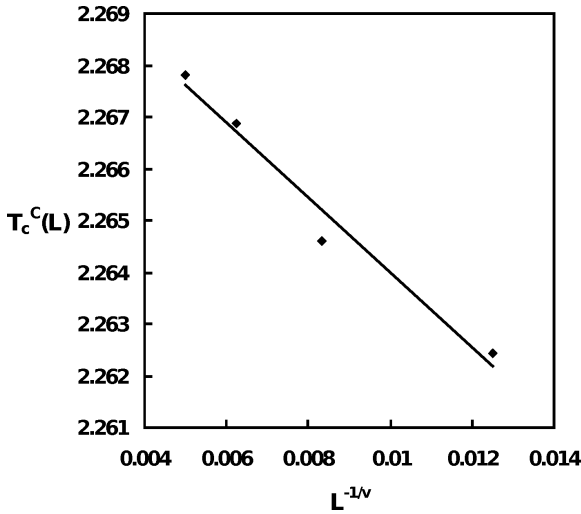


Fig. 3. The value of the infinite-lattice critical temperature for the specific heat  $C_L$ ,  $T_c = 2.271(1)$  obtained by extrapolating the straight line fitted to critical temperatures of the lattice with linear dimensions  $80 \leq L \leq 200$  as  $L \rightarrow \infty$ .

tion of the curves in Figure 2 for  $80 \leq L \leq 200$  gives the critical temperature of  $T_c = 2.287(6)$  at which the specific heat maxima occur when  $L \rightarrow \infty$ . The straight line fit in the plot of  $T_c^C(L)$  vs.  $L^{-1/\nu}$  also implies  $T_c = 2.271(1)$  as  $L \rightarrow \infty$ , seen in Figure 3. These results are in agreement with the value of the Creutz cellular automaton result of  $T_c = 2.263$  [17] and the theoretical prediction of  $T_c = 2.269$  [22]. In order to calculate the critical exponent for the specific heat we use the general relation for  $C_L$  at  $h = 0$  and  $t = 0$ . Thus, (6) reduces to the following form:

$$C_L \propto L^{\alpha/\nu}. \tag{9}$$

This relation is also used for the maxima of the finite lattices. By using the data of Table 1 in getting the log-log plots of  $C_L(T_c)$  and  $C_L^{\max}$  vs.  $L$ , the following values of  $\alpha$  are obtained:  $\alpha = 0.04(25)$  and  $\alpha_{\max} = 0.03(1)$ , the average of which is  $\alpha = 0.03(25)$ . These result is in agreement with  $\alpha = 0$  results predicted by the theory.

In Figure 4 we show the finite-size scaling plot of the specific heat. In this figure, not all of the data points for a given  $L$  fall on the finite-size scaling curve which is formed by the overlapping parts of the plots for different  $L$ . Since all the scaled quantities of  $C_L$  for different  $L$  values overlap above  $T_c$ , the finite-size scaling relations for  $C_L$  is valid only in the region above  $T_c$ . Therefore, this scaling for  $C_L$  is verified only in the region  $tL^{1/\nu} > 0$ , but not in the region  $tL^{1/\nu} < 0$ . It should

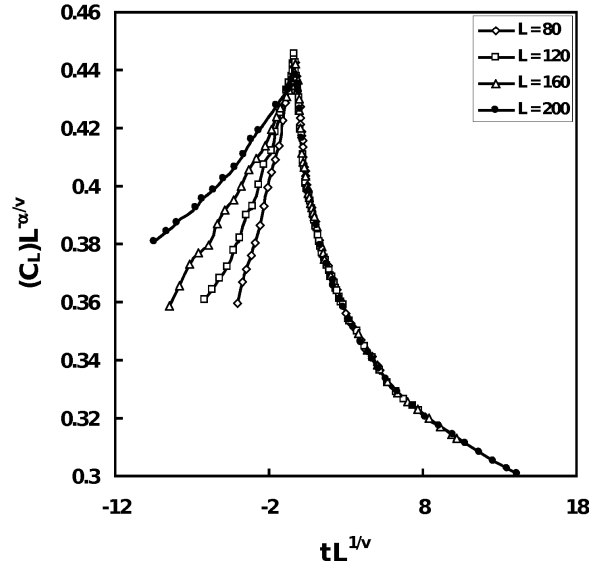


Fig. 4. The data for  $C_L$  shown in Figure 2 plotted vs the scaling variable  $tL^{1/\nu}$ , where  $T_c = 2.269(3)$ .

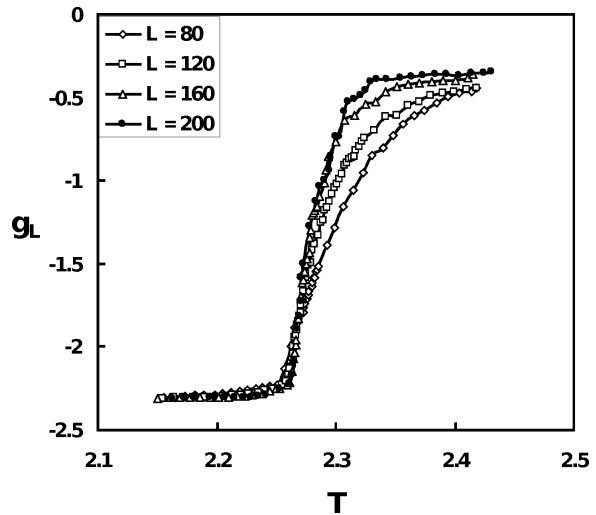


Fig. 5. Same as Figure 2, but for Binder parameter  $g_L$ .

be mentioned that the contribution to  $C_L$  from the regular part is not considered in this plot. That is, the values of the specific heat computed in the simulations are used directly in the plots.

The  $h = 0$  finite size renormalized coupling  $g_L$  (Binder parameter or Binder cumulant) introduced by Binder [16, 20, 21]

$$g_L = \frac{\langle s^4 \rangle_L}{\langle s^2 \rangle_L^2} - 3 = \left[ \frac{\chi_L^{(4)}}{L^4 \chi_L^4} \right]_{h=0}, \tag{10}$$

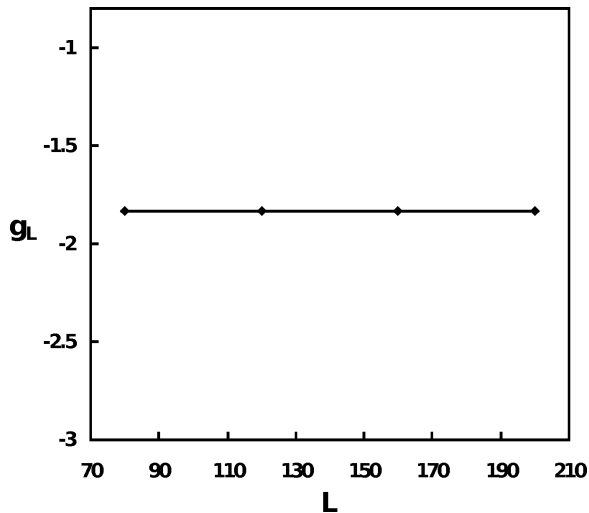


Fig. 6.  $L$ -dependence of the data in Figure 5.

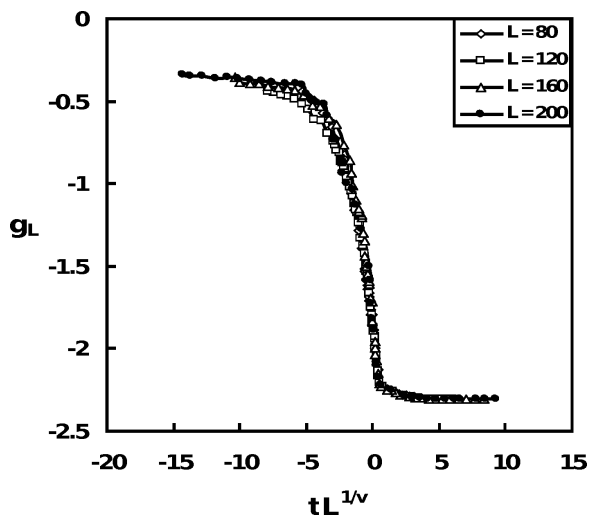


Fig. 7. Same as Figure 4, but for Binder parameter  $g_L$ .

where  $\chi_L$  is the susceptibility and  $\chi_L^{(4)}$  is the fourth field derivate; the subscript  $L$  denote the corresponding finite-size quantities. In the method of Binder [16, 20, 21], the critical point  $T_c$  is located by finding the common crossing point of plots of  $g_L$  vs. temperature for a range of different system sizes  $L$  [16, 20, 21]. The temperature variation of the Binder parameter for  $L = 80, 120, 160,$  and  $200$  is shown in Figure 5. In this figure, the intersection point of the curves for  $80 \leq L \leq 200$  gives  $T_c = 2.269(3)$  which is in good agreement with the theoretical prediction of  $T_c = 2.269$  [22]. From Figure 5 the values for the Binder parameter by using the finite-size

$L$	$g_L(T_c)$
80	-1.833(5)
120	-1.834(3)
160	-1.832(2)
200	-1.833(2)

Table 2. The values of the Binder parameter for the finite lattices.

lattices with the linear dimension  $L = 80, 120, 160,$  and  $200$  at  $T_c = 2.269(3)$  are calculated as  $g_L(T_c) = -1.833(5), g_L(T_c) = -1.834(3), g_L(T_c) = -1.832(2)$  and  $g_L(T_c) = -1.833(2)$ , respectively. From Figure 6 and Table 2 the value of the infinite lattice for the Binder parameter,  $g_L(T_c) = -1.834(11)$ , is obtained from the straight line fit of  $g_L(T_c) = -1.833(5), g_L(T_c) = -1.834(3), g_L(T_c) = -1.832(2),$  and  $g_L(T_c) = -1.833(2)$  versus  $L = 80, 120, 160,$  and  $200$ , respectively. This result is in good agreement with the Monte Carlo simulations results of  $g_L(T_c) = -(1.830 - 1.835)$  [23–27].

The finite-size scaling relation for the Binder parameter has the following form:

$$g_L = G(tL^{1/\nu}), \quad h \rightarrow 0, \quad L \rightarrow \infty, \quad (11)$$

where  $t > 0$  for  $T > T_c$  and  $t < 0$  for  $T < T_c$ . We illustrate  $g_L$  vs.  $tL^{1/\nu}$  in Figure 7. Since all the scaled quantities of  $g_L$  for different  $L$  values overlap above  $T_c$ , the finite-size scaling relations for  $g_L$  is valid only in the region above  $T_c$ . Therefore, this scaling for  $g_L$  is verified only in the region  $tL^{1/\nu} > 0$ , but not in the region  $tL^{1/\nu} < 0$ .

#### 4. Conclusion

Creutz cellular automaton computer simulations are a tool in scientific fields such as condensed-matter physics, including surface-physics and applied-physics problems (metallurgy and diffusion, etc.). With the increasing ability of this method to deal with quantum-mechanical problems such as quantum spin systems or many-fermion problems, it may become useful to answer some questions in the fields of elementary-particle and nuclear physics as well.

In this work, the two-dimensional Ising model is simulated on the Creutz cellular automaton using the finite-size lattices with the linear dimension  $L = 80, 120, 160,$  and  $200$  for the fractals obtained by using the model of diffusions-limited aggregation. Since all the scaled quantities of  $C_L$  and  $g_L$  for different  $L$  values overlap above  $T_c$ , the finite-size scaling relations for  $C_L$  and  $g_L$  are valid only in the region above  $T_c$ .

The computer used was an Intel<sup>(®)</sup> Core<sup>(™)</sup> 2 Duo CPU E6550 at 2.33 GHz. The CPU time invested was 1140 hours for all the simulations.

- [1] T. Vicsek, *Fractal Growth Phenomena*, World Scientific, Singapore 1990.
- [2] B. B. Mandelbrot and M. Frame, *Fractals*, Encyclopedia of Physical Science and Technology, Academic, San Francisco 1982.
- [3] B. B. Mandelbrot, *An Introduction to Multifractal Distribution Functions*, in *Random Fluctuations and Pattern Growth: Experiment and Models* (Ed. H. E. Stanley and N. Ostrowsky), Kluwer, Dordrecht 1988.
- [4] Z. Merdan and M. Bayirli, *Chin. Phys. Lett.* **22**, 2112 (2005).
- [5] S. R. Forrest and T. A. Witten, *J. Phys. A: Math. Gen.* **12**, L109 (1979).
- [6] T. A. Witten and L. M. Sander, *Phys. Rev. Lett.* **47**, 1400 (1980).
- [7] T. A. Witten and L. M. Sander, *Phys. Rev. B* **27**, 5686 (1983).
- [8] F. Family, B. R. Masters, and D. Platt, *Phys. D* **38**, 98 (1989).
- [9] L. Niemeyer, L. Pietrenerio, and H. J. Wiesmann, *Phys. Rev. Lett.* **52**, 1033 (1984).
- [10] M. Matsushita, M. Sano, H. Hanjo, and Y. Savada, *Phys. Rev. Lett.* **53**, 286 (1984).
- [11] H. Fijikawa and M. Matsushita, *J. Phys. Soc. Jpn.* **58**, 3875 (1989).
- [12] S. Y. Huang, X. W. Zou, Z. J. Tan, and Z. Z. Jin, *Phys. Lett. A* **292**, 141 (2001).
- [13] Z. J. Tan, X. W. H. Zou, and Z. Z. Jin, *Phys. Lett. A* **282**, 121 (2001).
- [14] M. Lattuada, H. Wu, and M. Mordibelli, *J. Coll. Interface Sci.* **268**, R106 (2003).
- [15] M. Creutz, *Ann. Phys.* **167**, 62 (1986).
- [16] V. Privman (Ed.), *Finite Size Scaling and Numerical Simulation of Statistical Systems*, World Scientific, Singapore 1990.
- [17] B. Kutlu and N. Aktekin, *J. Stat. Phys.* **75**, 757 (1994).
- [18] G. Y. Vichniac, *Phys. D* **10**, 96 (1984); Y. Pomeau, *J. Phys. A* **17**, L145 (1984); H. J. Hermann, *J. Stat. Phys.* **45**, 145 (1986); W. M. Lang, and D. Stauffer, *J. Phys. A* **20**, 5413 (1987).
- [19] Z. Merdan, B. Boyacıoğlu, A. Günen, and Z. Sağlam, *Bull. Pur. Appl. Sci. D* **22**, 95 (2003); Z. Merdan, A. Günen, and G. Mülazımoğlu, *Int. J. Mod. Phys. C* **16**, 1269 (2005); Z. Merdan, A. Günen, and Ş. Çavdar, *Phys. A* **359**, 415 (2006); Z. Merdan, R. Erdem, *Phys. Lett. A* **330**, 403 (2004); Z. Merdan and M. Bayırlı, *Appl. Math. and Comp.* **167**, 212 (2005); Z. Merdan, A. Duran, D. Atille, G. Mülazımoğlu, and A. Günen, *Phys. A* **366**, 265 (2006); Z. Merdan and D. Atille, *Phys. A* **376**, 327 (2007); Z. Merdan and D. Atille, *Mod. Phys. Lett. B* **21**, 215 (2007); G. Mülazımoğlu, A. Duran, Z. Merdan, and A. Günen, *Mod. Phys. Lett. B* **13**, 1329 (2008).
- [20] N. Aktekin, in: *Annual Reviews of Computational Physics*, Vol. VII, (Ed. D. Stauffer), World Scientific, Singapore 2000.
- [21] K. Binder, M. Nauenberg, V. Privman, and A. P. Young, *Phys. Rev. B* **31**, 1498 (1985).
- [22] K. Huang, *Statistical Mechanics*, 2. Ed. John Wiley and Sons, New York 1987.
- [23] A. D. Bruce, *J. Phys. A* **18**, L873 (1985).
- [24] T. W. Burkhardt and B. Derrida, *Phys. Rev. B* **32**, 7273 (1985).
- [25] H. Saleur and B. Derrida, *J. Physique* **46**, 1043 (1985).
- [26] P. Di Francesco, H. Saleur, and J.-B. Zuber, *Nucl. Phys. B* **290**, 527 (1987).
- [27] P. Di Francesco, H. Saleur, and J.-B. Zuber, *Europhys. Lett.* **5**, 95 (1988).